On differential-equation-based-neural-networks on manifolds

Hirotada Honda[1], Nguyen Tuan[2], Takashi Sano[1], and Shugo Nakamura[1]
[1]Faculty of Information and Networking for Innovation and Design, Toyo University
[2]FPT Consulting Japan, FPT Software
e-mail : honda.hirotada@iniad.org

1 Inroduction

Recently, it is pointed out that the 2nd order Neural ODE (NODE) expresses the broader representativeness than the 1st order one [1], and a large number of works following this direction have been reported. In particular, the first remarkable argument was that the 1st order NODE on $\mathbb{R}$ cannot realize a function of the form $f(x) = -x$ [2]. In this talk, we consider this problem as a map on an orientable manifold and the problem of maps that can be realized as *flows* on manifolds.

2 Notations

Hereafter, d and r denote integers that satisfy $d, r \geq 1$. For a manifold M, $\mathrm{Diff}^r(M)$ denotes a set of diffeomorphisms of C^r class from M to itself. Similarly, $\mathrm{Diff}^r_0(M)$ denotes a set of C^r diffeomorphisms that are isotopic to the identity on M. A st of vector fields on M is denoted as $\chi(M)$. For topological spaces X_i $(i = 1, 2, 3)$ and a continuous map $\phi : X_1 \times X_2 \to X_3$, we define its adjoint map $\mathrm{ad}(\phi)(x_1) : x_2 \to x_3$ by $\mathrm{ad}(\phi)(x_1)(x_2) = \phi(x_1, x_2)$, where $x_i \in X_i$ $(i = 1, 2)$.

3 Flows on Euclidean spaces

Theorem 1. *Let $T > 0$ and suppose that $f \in \mathrm{Diff}(\mathbb{R}^d)$ is given. Then, we can take maps $s : \mathbb{R}^d \to \mathbb{R}^{d+1}$, $pr : \mathbb{R}^{d+1} \to \mathbb{R}^d$, and a vector field $X \in \chi(\mathbb{R}^{d+1})$, whose corresponding flow is $\phi_{T,X} : \mathbb{R}^{d+1} \to \mathbb{R}^{d+1}$, with which we can satisfy $pr \circ \phi_{T,X} \circ s = f$.*

The proof of this theorem will be given in our talk, in which we shall make use of the fact that in case of Euclidean spaces, $\mathrm{Diff}(\mathbb{R}^d)$ coincides with $\mathrm{Diff}_0(\mathbb{R}^d)$ [3]. We note that this gives the explanation and the minimum dimension of the Euclidean space with which we can realize the orientation-reversing map.

4 Flows on manifolds

In case of a general manifold, $\mathrm{Diff}_0(M)$ is a strict subset of $\mathrm{Diff}(M)$. Regarding $\mathrm{Diff}_0(M)$, however, we can realize its elements as flows if we allow all possible vector fields [4, 5]. We can restrict the type of the vector fields [5, 6].

Theorem 2. *Let M be a compact, smooth, and orientable manifold and $\triangle$ be a bracket-generating distribution on M. Then, any $f \in \mathrm{Diff}_0(M)$ can be realized as a flow on M; that is, by considering a system of time-dependent ordinary differential equations of the form*

$$\begin{cases} \dot{q} = \sum_{i=1}^{k} u_i(t, q) h_i(q) & \text{in } t \in (0, T), \\ q\big|_{t=0} = \xi \in M, \end{cases}$$

where $\{h_i\}_{i=1}^k \subset \triangle$ *and* $u_i (i = 1, \ldots, k)$ *are feedback controls that should be taken appropriately, we are able to attain* $q(T; \xi) = f(\xi)$.

However, the statement above is limited only to maps in $\mathrm{Diff}_0(M)$. We now consider realizing a wider range of maps on M as a structure group of a fiber bundle under some conditions. For the sake of simplicity, we hereafter take $T = 1$ as the terminal moment of the flow. For a fiber bundle P, we denote the projection from P to its fiber F as $pr_2 : P \to F$.

Theorem 3. *Let* M *be a* d*-dimensional closed, connected, smooth orientable manifold that admits an orientation-reversing diffeomorphism. Moreover, suppose that all orientation-preserving maps are isotopic, and the same applies to all orientation-reversing maps. Then, we have a fiber bundle* P *of dimension* $d + 1$ *with base space* S^1 *with the following properties.*

(i) *The fiber of* P *is* M*;*

(ii) *For any* $f \in \mathrm{Diff}(M)$*, we can take a function* $s : M \to S^1$*, vector field* $X_f \in \chi(P)$ *and a corresponding flow* $\sigma_{X_f} : P \to P$ *with which we can define a coordinate function* $\phi_\alpha : \pi^{-1}(U_\alpha) \to U_\alpha \times M$*, where* $\{U_\alpha\}_\alpha$ *is a family of open coverings of* S^1*, and an adjoint map* $\mathrm{ad}_{s(x)}^{\sigma_{X_f}}$ *depending on* $s(x)$ *and* σ_{X_f} *which satisfy* $\mathrm{ad}_{s(x)}^{\sigma_{X_f}}(pr_2 \circ \phi_\beta \circ \phi_\alpha^{-1}) = f$.

We will give the proof of this theorem by using mapping torus [7, 8].

謝辞 This work was supported by Toyo University Top Priority Research Program.

参考文献

[1] Massaroli, S. et al., Dissecting Neural ODEs, Advances in Neural Information Processing Systems, 33(2020), 3952–3963.

[2] Dupont, E. Doucet, A., and Teh, Y.W., Augmented Neural ODEs, `https://arxiv.org/abs/1904.01681`.

[3] Milnor, W., Topology from the Differentiable Viewpoint, Revised edition, Princeton University Press, 1997.

[4] Thurston, W., Foliations and groups of diffeomorphisms, Bull. Amer. Math. Soc. 80 (1974), , 304–307.

[5] Agrachev, A. A. and Caponigro, M., Controllability on the group of diffeomorphisms, Annals of the Institute Henri Poincaré C, Non-linear analysis, 26 (2009), 2503–2509.

[6] Caponigro, M., Orientation preserving diffeomorphisms and flows of control-affine systems, IFAC Proceedings, 44(2011), 8016–8021.

[7] Robinson, R. C. and Robinson, C., Dynamical Systems: Stability, Symbolic Dynamics, and Chaos, 2nd edition, CRC Press, 1998.

[8] Suda, T. A categorical view of Poincaré maps and suspension flows, Dynamical Systems, 37(2022), 159–179.

囲い込みニューラルネットワークによる内部包含物の同定と数値実験

井手 貴範 [1], Samuli Siltanen[2]
[1] 城西大学 理学部 数学科, [2]University of Helsinki, Faculty of Science, Department of Mathematics and Statistics
e-mail : tide@josai.ac.jp

1　はじめに

Electrical Impedance Tomography(EIT) は物体の表面に電圧を与えた時，物体表面に発生した電流の計測値から内部包含物の位置を画像再構成する非破壊検査法として知られている．EIT は次の偏微分方程式の逆問題として記述することができる [1]．$\mathbb{R}^2$ 内の物体 Ω（有界集合）の電気伝導度を $\sigma = \sigma(x, y)$，電圧のポテンシャルを $u = u(x, y)$ とすると次の偏微分方程式が成り立つ．

$$\begin{cases} \nabla \cdot \sigma \nabla u = 0 \ in \ \Omega, \\ u = f \ on \ \partial\Omega. \end{cases} \tag{1}$$

ここで，n を境界 $(\partial\Omega)$ 上の単位法線ベクトルとし，以下のような Dirichlet–Neumann 写像を与える．

$$\Lambda_\sigma : f \to \sigma \frac{\partial u}{\partial n}\bigg|_{\partial\Omega}. \tag{2}$$

また，電気伝導度を次のように与える．

$$\sigma(x, y) = 1 + \chi_D(x, y)h(x, y). \tag{3}$$

ここで，$D \subset \Omega$ を内部包含物の集合とし，次式が成り立つとする．

$$\chi_D(x, y) = \begin{cases} 1, \ (x, y) \ \in \ D \\ 0, \ (\text{その他}) \end{cases}. \tag{4}$$

この時，「Dirichlet–Neumann 写像 Λ_σ から内部包含物 D を再構成できるのか?」という問題を解くために，囲い込み法とニューラルネットワークを組み合わせた手法と数値実験の結果を紹介する．

2　囲い込み法

囲い込み法の概要を述べる [2]．Ω を単位円盤とし，内部包含物 $D \subset \Omega$，単位ベクトル $\omega \in S^1$ とする．$\omega^\perp$ は反時計回りに直角に回転したベクトルとする．この時，$\omega \cdot \omega^\perp = 0$ をみたす．$\forall \tau > 0$, $x \in \mathbb{R}^2$ に対して，次の指数関数を定義する．

$$f_\omega(x, \tau) := e^{\tau x \cdot \omega + i\tau x \cdot \omega^\perp}. \tag{5}$$

この時，支持関数 (support function) を次式で定義する．

$$h_D(\omega) := \sup_{x \in D} x \cdot \omega. \tag{6}$$

次に指示関数 (indicator function) を次式で定義する．

$$I_\omega(\tau) := \int_0^{2\pi} ((\Lambda_\sigma - \Lambda_1)\overline{f_\omega(\cdot, \tau)}|_{\partial\Omega})(\theta) f_\omega(e^{i\theta}, \tau) d\theta. \tag{7}$$

ここで，Λ_1 は導電率が 1 の時の Dirichlet–Neumann 写像とする．この時，十分大きな τ に対して，支持関数は

$$h_D(\omega) = \lim_{\tau\to\infty} \frac{\log|I_\omega(\tau)|}{2\tau} \tag{8}$$

となる．これまで，上式を用いて内部包含物の再構成の数値実験の研究が行われていた [3].

3　囲い込みニューラルネットワーク

囲い込みニューラルネットワークの概要を述べる [4]．囲い込みニューラルネットワークは入力データとして以下を用いる．

$$\begin{aligned} &\omega_j = [\cos\theta_j, \sin\theta_j]^T \\ &\theta_j = 2\pi(j-1)/N,\ j = 1, \cdots, N. \end{aligned} \tag{9}$$

τ は $1.5 \le \tau \le 4.5$ とし刻み幅は 0.5 とする．これは次式となる．

$$\tau_l = 1 + \frac{l}{2},\ l = 1, \cdots, 7. \tag{10}$$

次に，これらの入力データを用いて，τ_l と支持関数から得られる次の 2 次元平面上の値を計算する．

$$(\tau_l, \frac{1}{2}\log|I_{\omega_j}(\tau_l)|) \in \mathbb{R}^2,\ l = 1, \cdots, 7. \tag{11}$$

この値を用いて畳み込みニューラルネットワークを計算することで内部包含物を画像再構成する．

4　数値実験

数値実験の結果は講演時に紹介する．

参考文献

[1] A.P. Calderón, On an inverse boundary value problem, Seminar on Numerical Analysis and its Applications to Continuum Physics (1980), 65–73.

[2] M. Ikehata, Reconstruction of the support function for inclusion from boundary measurements, Journal of Inverse and Ill–Posed Problems, 8 (2000), 367–378.

[3] M. Ikehata and S. Siltanen, Numerical method for finding the convex hull of an inclusion in conductivity from boundary measurements, Inverse Problems 16 (2000), 1043-1052.

[4] S. Siltanen, T. Ide, Electrical impedance tomography, enclosure method and machine learning, Proceeding of 2020 IEEE 30th International Workshop on Machine Learning for Signal Processing, (2020), 1–6.

1 次元保存則のためのラグランジュ移動メッシュ法

Kharisma Surya Putri[1], 水落樹[2], Niklas Kolbe[3], 野津裕史[4]
[1,2,4]金沢大学, [3]RWTH Aachen University
e-mail : kharismasp@stu.kanazawa-u.ac.jp

1　保存型移流拡散問題

$\Omega = (a,b) \subset \mathbb{R}$ $(a < b)$ を有界領域, $\Gamma := \partial\Omega$ を Ω の境界, $n : \partial\Omega \to \mathbb{R}$ を外向き単位法線, T を正の定数とする. 速度 $u\colon \Omega \times (0,T) \to \mathbb{R}$ と初期データ $\phi^0\colon \Omega \to \mathbb{R}$ は与えられた関数であり, $\nu > 0$ は拡散係数とする. ここに, $u \in C^0([0,T]; W_0^{1,\infty}(\Omega))$ を仮定する. 次の 1 次元保存型移流拡散問題：

$$\frac{\partial \phi}{\partial t} + \nabla \cdot (u\phi) - \nu \Delta \phi = 0, \quad (x,t) \in \Omega \times (0,T), \tag{1a}$$

$$\nu \frac{\partial \phi}{\partial n} - \phi u \cdot n = 0, \quad (x,t) \in \Gamma \times (0,T), \tag{1b}$$

$$\phi = \phi^0, \quad (x,t) \in \Omega \times \{0\}, \tag{1c}$$

をみたす関数 $\phi : \Omega \times (0,T) \to \mathbb{R}$ を求めよ, を考える.

2　ラグランジュ・ガレルキン移動メッシュ（LGMM）法

問題 (1) の基本的な離散化は時間 2 次精度質量保存ラグランジュ・ガレルキン (LG) 法 [2] を用いて行う. LG 法は, 一般に, 無条件安定性, 係数行列の対称性などの長所が知られており, 移流が支配的な問題のための強力な手法のひとつある. しかしながら, 鋭いスパイクが現れるような凝集現象を捉えようとする場合, 固定メッシュを用いる LG 法では, 振動が現れることがある (図 1 参照).

LG スキームは, 速度場による上流点を求め, 前の時刻の数値解の値を参照する. 我々の基本的なアイデアは, 質量輸送に基づくアプローチ [1] を参照し, メッシュを速度場に沿って移動させることである. メッシュを移動することにより, 数値計算において上流点を容易に特定し, また, 補間誤差を軽減する可能性がある.

時間 $t \in [0,T]$ に対して, $\mathcal{T}_h(t) = \{K_i(t)\}_{i=1}^{Np-1}$ を時間依存のメッシュ, $\{P_i(t)\}_{i=1}^{N_p} \subset \overline{\Omega}$ を節点の座標の集合, $\{\phi_i(x,t)\}_{i=1}^{N_p}$ を P1-基底関数の集合とする. 初期節点座標の集合 $\{P_i^0\}_{i=1}^{N_p} \subset \overline{\Omega}$ が与えられたとする. $a = P_1^0 < P_2^0 < ... < P_{N_p}^0 = b$ を仮定する. 次の常微分方程式に支配される問題：

$$\frac{dP_i}{dt}(t) = u\big(P_i(t),t\big) + \nu \sum_{K(t) \ni P_i(t)} [\nabla \varphi_i(t)]_{|K(t)}, \qquad i = 2,\dots,N_p - 1,\ t \in (0,T), \tag{2a}$$

$$P_1(t) = a, \quad P_{N_p}(t) = b, \qquad t \in (0,T), \tag{2b}$$

$$P_i(t) = P_i^0, \qquad i = 1,\dots,N_p,\ t = 0, \tag{2c}$$

をみたす $\{P_i(t) \in \bar{\Omega}; i = 1,...,N_p, t \in (0,T)\}$ を求めよ, の解を用いてメッシュ (節点) を移動する.

本研究では, LG 法と上記のメッシュ移動法の組み合わせたラグランジュ・ガレルキン移動メッシュ (LGMM) 法 [3] を提案する.

3　理論結果

我々の LGMM 法の数学的解析を行い, 以下の 4 つの結果を得た. 以下では, 時間刻み幅 Δt は $\Delta t |u|_{C(W^{1,\infty})} \le 1/8$ の条件をみたすとする. 問題 (2) の後退オイラー法を基礎とした近似解を単に

問題 (2) の近似解と書く (詳細は [3] 参照).

定理 1 (メッシュが重ならない条件)**.** $\{P_i^n \in \overline{\Omega}; i = 1, \ldots, N_p, n = 1, \ldots, N_T\}$ を問題 (2) の近似解とする. このとき, $P_i^n < P_j^n$ $(i < j,\ i, j \in \{1, ..., N_p\}, n \in \{0, \ldots, N_T\})$ が成立する.

定理 2 (質量保存性)**.** *LGMM* 法の解を $\{\phi_h^n\}_{n=0}^{N_T} \subset \Psi_h$ とする. このとき, $n = 0, 1, \ldots, N_T$ に対して, $\int_\Omega \phi_h^n \, dx = \int_\Omega \phi_h^0 \, dx$ が成り立つ.

定理 3 (安定性)**.** *LGMM* 法の解を $\{\phi_h^n\}_{n=0}^{N_T} \subset \Psi_h$ とする. このとき, h と Δt に依存しない $C > 0$ が存在し, 不等式 $\|\phi_h\|_{\ell^\infty(L^2)} + \sqrt{\nu}\|\nabla\phi_h\|_{\ell^2(L^2)} \le C\|\phi_h^0\|$ が成り立つ.

定理 4 (誤差評価)**.** 問題 (1) の解 ϕ は, $\phi \in Z^3 \cap H^2(0, T; H^2(\Omega)) \cap H^1(0, T; H^3(\Omega))$ をみたすとする. 初期時刻のメッシュを用いたラグランジュ補間による関数 $\phi_h^0 = \Pi_h^0 \phi^0 \in \Psi_h^0$ に対する *LGMM* 法の解を $\{\phi_h^n\}_{n=0}^{N_T}$ とする. このとき, h と Δt に依存しない定数 $C > 0$ が存在して, $\|\phi_h - \phi\|_{\ell^\infty(L^2)} + \sqrt{\nu}\|\nabla(\phi_h - \phi)\|_{\ell^2(L^2)} \le C(\Delta t^2 + h^2)\|\phi\|_{Z^3 \cap H^2(H^2) \cap H^1(H^3)}$ が成り立つ.

4 数値結果

提案した LGMM 法の検証のために, LG 法と LGMM 法を使用して問題 (1) の数値計算を行った. 次の具体的な問題を設定する: $\Omega = (-1, 1)$, $T = 2$, $u(x, t) = \sin(2\pi x), \nu = 10^{-5}$, および $\phi^0(x) = \exp[-(1 - \cos x)/0.01]$. 図 1 において, 固定メッシュを用いた LG 法と LGMM 法の結果を比較する. 固定メッシュ LG 法が振動する解をもたらす一方で, LGMM 法が凝集現象を高精度に捉えていることが観察される.

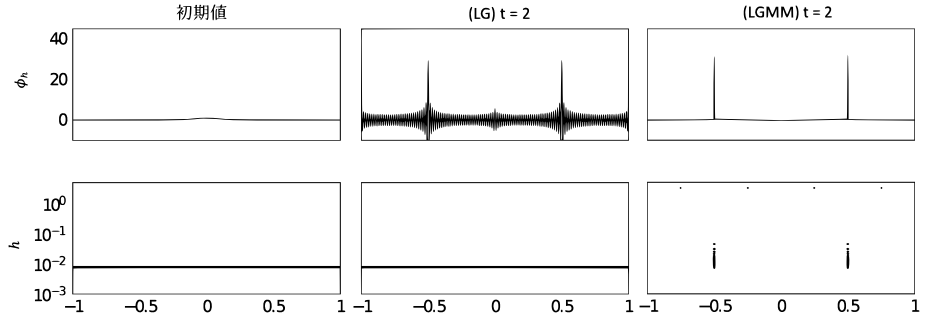

図 1. 初期値 $t = 0$ (左), 固定メッシュ LG 法 $t = 2$ (中央), LGMM 法 $t = 2$ (右) の結果

参考文献

[1] J.A. Carrillo, N. Kolbe, and M. Lukacova–Medvid'ova. A hybrid mass transport finite element method for Keller-Segel type systems. *J. Sci. Comput.* **80**, 1777–1804, 2019.

[2] K. Futai, N. Kolbe, H. Notsu, and T. Suzuki. A mass-preserving two-step Lagrange-Galerkin scheme for convection-diffusion problems. *J. Sci. Comput.* **92**, 37, 2022.

[3] K.S. Putri, T. Mizuochi, N. Kolbe, and H. Notsu. Error estimates for first- and second-order Lagrange-Galerkin moving mesh schemes for the one-dimensional convection-diffusion equation. Submitted. arXiv:2402.14691[math.NA].

On a method of uniform point distributions

Prapapit CHUTIMANTANON[1], Shigetoshi YAZAKI[2]
[1] 明治大学大学院理工学研究科, [2] 明治大学理工学部
e-mail : chutimantannthp@gmail.com

1 Introduction

Random point distributions are widely recognized and practical methods for addressing various problems. Although these distributions intuitively spread points uniformly, they are generally different. Consequently, many researchers have investigated the so-called low-discrepancy or quasi-random sequences, which can be generated by several ideas to achieve uniform point distribution. These sequences have applications in numerous fields, including Physics, Finance, numerical integration, etc. The aim of this study is to measure uniformity using some energies and, conversely, to identify a pattern of point distribution for a given energy.

2 Mathematical background

The Koksma-Hlawka inequality provides an upper bound for the error in numerical integration using a sequence $\omega = (x_n)_{n=0}^{\infty}$ in $[0,1]^s$, relating it to the star discrepancy $D_N^*(\omega)$ which measures the uniformity of the sequence, and the variation V(f) as following

$$\left| \int_{[0,1]^s} f(x)\, dx - \frac{1}{N} \sum_{n=0}^{N-1} f(x_n) \right| \leq V(f) D_N^*(\omega),$$

where $N \in \mathbb{N}$ and s is the dimension of $f(x)$. By the conditions of this inequality, $D_N^*(\omega)$ should be small since $V(f)$ remains constant. This is why we are interested in low-discrepancy sequences: the first N terms of such sequences have low discrepancy. Examples of low-discrepancy sequences include the van der Corput sequence, the Halton sequence, and the Hammersley sequence.

2.1 van der Corput sequences

Let b be a natural number and greater than 1, every non negative number n can write the its representation in a base b as

$$n := \sum_{i=0}^{\infty} d_i b^i = d_0 + d_1 b^1 + d_2 b^2 + ...,$$

where $d_i \in \{0, 1, 2, ..., b-1\}$. After that, to inverse an non negative number n in an interval $[0, 1)$ by a function

$$\phi_b(n) := \sum_{i=0}^{\infty} \frac{d_i}{b^{i+1}} = \frac{d_0}{b^1} + \frac{d_1}{b^2} + \frac{d_2}{b^3} + ...,$$

therefore, the van der Corput sequence in base b is $\phi_b(n)_{n=0}^{\infty} = (\phi_b(0), \phi_b(1), ...)$.

2.2 Halton sequences

Let $b_1, b_2, ..., b_s$ be natural numbers and greater than 1, s be a natural number and n be an non negative number. The representation of n in a base b_j as

$$n := \sum_{i=0}^{\infty} d_i b_j^i = d_0 + d_1 b_j^1 + d_2 b_j^2 + ...,$$

where $d_i \in \{0, 1, 2, ..., b_j - 1\}$. Then, inversing an non negative number n of each base b_j in an interval $[0, 1)$ by a function

$$\phi_{b_j}(n) := \sum_{i=0}^{\infty} \frac{d_i}{b_j^{i+1}} = \frac{d_0}{b_j^1} + \frac{d_1}{b_j^2} + \frac{d_2}{b_j^3} + ...$$

Hence, the Halton sequence in base $b_1, ..., b_s$ is $(\phi_{b_1}(n)_{n=0}^{\infty}, \phi_{b_2}(n)_{n=0}^{\infty}, ..., \phi_{b_s}(n)_{n=0}^{\infty})$ or in the form of $((\phi_{b_1}(0), \phi_{b_2}(0), ..., \phi_{b_s}(0)), (\phi_{b_1}(1), \phi_{b_2}(1), ..., \phi_{b_s}(1)), ...)$

2.3 Hammersley sequence

Hammersley sequences are similarly to Halton seqnces, but they change the last position of their bases $(\phi_{b_1}(n)_{n=0}^{\infty}, \phi_{b_2}(n)_{n=0}^{\infty}, ..., \{\frac{n}{N}\}_{n=0}^{\infty})$ where they have s dimensions and N is the first number terms which we are interested in.

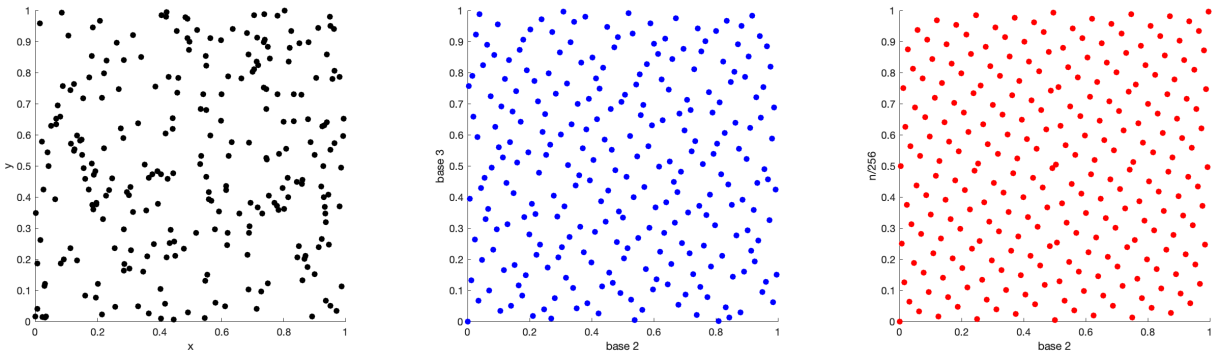

図 1. The random sequence is shown in 100 black points, the Halton sequence in base 2 and base 3 is shown in 100 blue points, and the Hammersley sequence in base 2 and base n/100 is shown in 100 red points.

